OPTIMIZING MISSION SCIENCE: THE READ-OUT MODES OF THE EPIC FOR X-RAY ASTRONOMY

C. MUSSO[1,2]*, L. CHIAPPETTI[1] and G.F. BIGNAMI[1,3]
[1] *IFCTR-CNR, v. Bassini 15, I-20133, Milano, Italy*
[2] *Alenia Spazio S.p.A., c.so Marche 41, I-10146, Torino, Italy*
[3] *Dipartimento di Ingegneria Industriale, Università di Cassino, v. Zamosch 43, I-03043, Cassino, Italy*

(Received 13 October 1994; accepted 5 June 1995)

Abstract.
The European Photon Imaging Camera (EPIC), which will fly onboard the ESA X-ray Multi Mirror (XMM) satellite, is an X-ray imaging and spectroscopy instrument based on CCD technology. The detectors placed in the three focal plane cameras will provide images and spectra in the energy band from 0.1 to ~ 10 keV. In order to observe sources within a wide range of intensities, several read-out modes have been planned for the detectors. Each of these modes works well up to some value of the intensity of the source, above which pile-up, i.e. the interaction of more than one photon with the same pixel or two adjacent pixels, in a single frame, becomes relevant.

After a brief description of the read-out modes, the simulations performed to establish a quantitative criterion for the limiting rates are presented. The results are discussed and compared with those reported by Chiappetti (1994a). Finally, some comments are made on the impact of these results on the scientific objectives of the mission.

1. Introduction

The X-ray Multi-Mirror (XMM) telescope mission is one of the four 'cornerstone' projects in the ESA long-term programme for space science. It will provide high X-ray throughput in the spectral range from 0.1 to ~ 10 keV and the key instrument in reaching this objective is the European Photon Imaging Camera (EPIC) (Bignami et al. 1989).

EPIC consists of 3 cameras based on Charge Coupled Device (CCD) technology (Lumb et al. 1991), as the focal plane detectors of three grazing-incidence telscopes. The effective area of the whole instrument will be of about 6000 cm^2 at 2 keV and 3000 cm^2 at 7 keV, with a limiting flux of $\sim 2 \times 10^{-15}$ $erg\ cm^{-2}\ s^{-1}$ for a point source, allowing medium spatial resolution (~ 30" HEW, but a point source location in the 5"-10" range) and broadband (0.1 to 10 keV) spectroscopy with resolving power $E/\Delta E$ ($FWHM$) between 5 and 60.

The cameras will be of two different types: the first is based on MOS technology (Turner 1994), and will be in the focus of two of the three telescopes; the second one is based on pn technology (Strüder 1994), and will be in the focus of the third telescope. The MOS cameras are made by seven

* e-mail: musso@ifctr.mi.cnr.it

Experimental Astronomy **6**: 235–248, 1995.
© 1995 *Kluwer Academic Publishers. Printed in the Netherlands.*

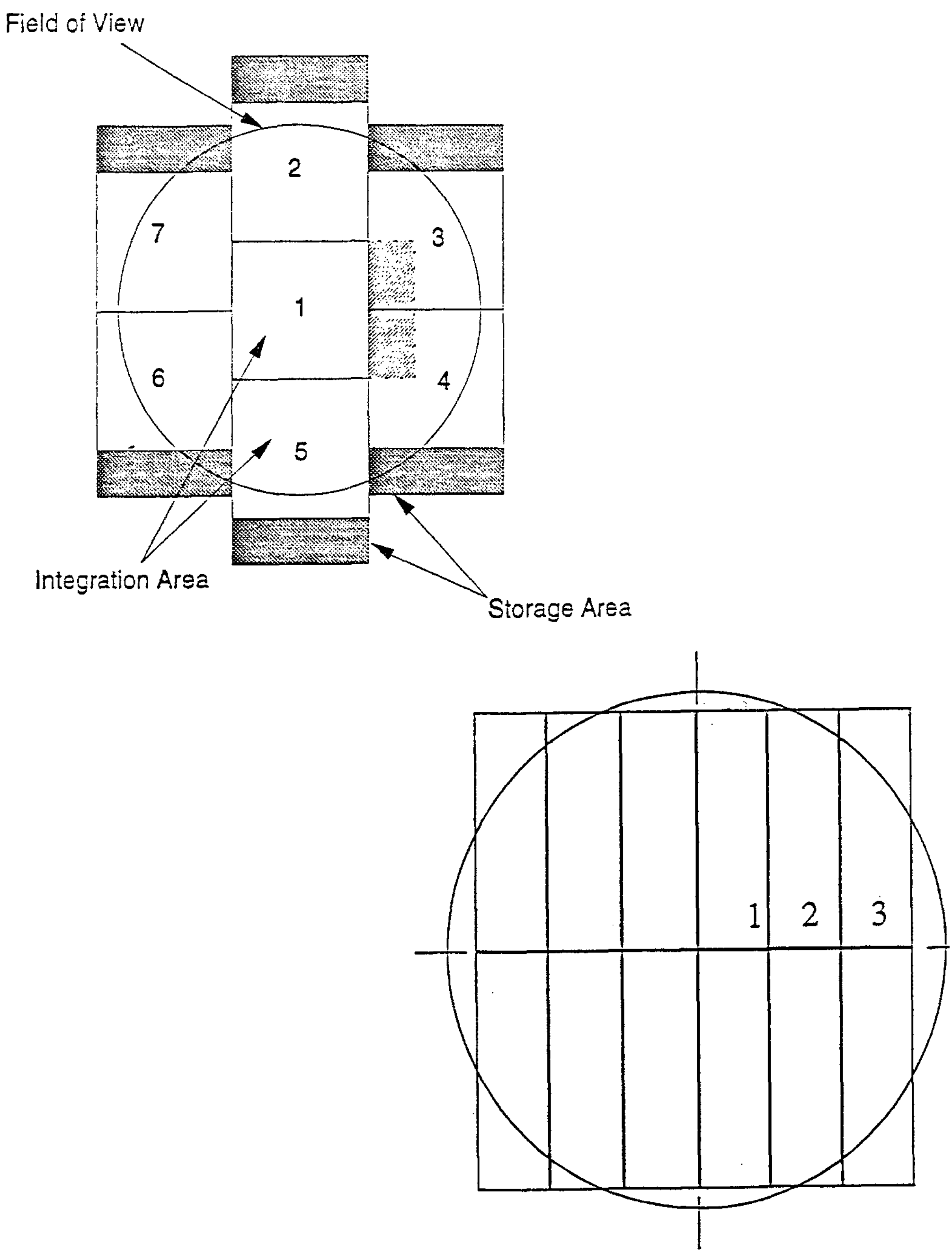

Fig. 1. Focal plane arrangement for MOS and pn CCDs.

front-illuminated CCDs, each of them composed by 600×600 pixels with a size of $(40\ \mu m)^2$, plus a shielded frame store region of 600×600 pixels of $40\ \mu m \times 12 \mu m$ size. The pn camera consists in twelve back-illuminated CCDs composed by 64×200 pixels with a size of $(150\ \mu m)^2$. The chip configuration for the two cases is shown in Fig.1. In both cases no mechanical shutter will be operational during observations.

In order to accumulate good spectra with CCD devices, it is necessary that only one photon interacts with any one pixel, during a single frame exposure time. If this is not the case, the read-out will interpret the effect of more than one photon as a single event of higher energy (pile-up), and the resulting spectrum will be degraded. This fact sets a constraint on the intensity of the observable sources (limiting rate), and requires the development of different read-out modes for different exposure times, in order to observe the widest possible range of source fluxes.

2. Read-out modes

The data collection in EPIC is controlled by a few parameters which are programmable via telecommand, such as the frame time, the window size and the number of output nodes, whose combination define the different read-out modes.

In order to fully exploit the EPIC capabilities, not only image modes but also some non-standard timing modes have been planned (see Sarra and Bignami 1993).

An important difference between the two types of CCDs, regarding the read-out modes, is the presence of a shielded region in the MOS chips, which permits storage of the data and read-out during the integration of a new frame. This option is not available for the pn case in which, however, the smaller number of larger pixels are read in parallel by a CMOS Amplifier and Multiplexing chip (CAMEX), resulting in a faster read-out process. The serial register of each MOS CCD is connected with one (or two) read-out node(s).

The operating modes currently studied are: Frame Store (FS), Window Frame Store (WFS), Refresh Frame Store (RFS) and Timing (MT) for the MOS CCDs (Pigot 1993); Full Frame (FF), Large Window (LW), Small Window (SW), Timing (PT) and Burst (B) for the pn CCDs (Chiappetti et al. 1993).

In the following we briefly describe how the different read-out modes operate. All the time parameters used in the simulation programs rely on the following "clock tic" assumptions. For the MOS case three basic times have been used: row shift is 2 μs, pixel shift is 1 μs, and pixel sampling is 5 μs; on the other hand, for the pn case the two basic times are a 1 μs row shift and a 20 μs parallel row read.

At the present time, EPIC CCDs are in development and the first calibration tests are currently in progress.

2.1 Frame Store (MOS imaging mode)

This is the basic configuration for MOS imaging, even if it is formally a variant of the WFS configuration, with window size corresponding to the whole chip. The typical frame time is 2.2 s with 1 node, and 1.1 s with 2 nodes. The integrated image is shifted in the store region, where the read-out process is performed; during the read-out time another image is accumulated.

2.2 Window Frame Store (MOS imaging mode)

The size and position of the read-out region (window) in a single given chip are free parameters. Noting that the HEW of a point source is 27 pixels, as a baseline value we choose a window of 100×100 pixels, encompassing a region larger than 3 HEWs, which allows also background estimation. In this case, the frame time is 0.11 s. The integrated image is shifted in the store region, then the out-of-window rows are cleared out to the serial register, without sampling; the window rows are read-out as follows: unwanted columns without sampling, then required area, then remaining area with unwanted columns; finally, remaining unwanted rows, if any, are cleared out again. The other chips are operated in the FS mode.

2.3 Refresh Frame Store (MOS imaging mode)

In this case, again for one particular chip, the frame time is 1.1 s (2 nodes), but the integration time is programmed to be less than the read-out time. The image and the store sections are clocked together, so that the image section is transferred into the store section, and the store section, without sampling, into the serial register, which is cleared. Then two operations are performed in parallel: (1) the read-out of the store section is performed during a time $T_{read-out}(= T_0 + T_{transfer} + T_{int})$; (2) during this time, in the image section, dummy data are collected (T_0) and then transferred in the first empty lines of the store section ($T_{transfer}$) without sampling; finally, relevant data are collected (T_{int}). In this way the duty cycle is $T_{int}/T_{read-out}$; if $T_{int} = 0.06s$ the duty cycle is 5.76%. The other chips are operated in the FS mode.

2.4 Timing (MOS timing mode)

This can also be called "Fast Window" mode. We choose a window of 54×54 pixels (2 HEWs). The image and the store sections are clocked together, so that the last image line is transferred in the store section and the last stored line into the serial register. Then two operations are performed in parallel: (1) the next 53 lines of the image section are quickly summed in the first line of the store section (i.e. the line of the store section next to the image section), each pixel of this line being the sum of the 54 pixels of the above column, and (2), after quick clearing of the first irrelevant pixels of the serial register without reading them, the read-out of the 54 pixels corresponding to the analysed columns is performed, followed by the clearing of the serial register up to the window region: the read-out time is $54 \times 6\ \mu s + 546 \times 1\ \mu s = 0.87\ ms$. This procedure results in the collection of a light curve with spatial information only on one axis, but with a time resolution of less than one millisecond.

2.5 *Full Frame (pn imaging mode)*

This is the standard configuration for pn imaging. The 12 CCDs are read-out sequentially; since each CCD needs 4 ms to be read-out, the frame time results to be 0.048 s, with an integration time of 44 ms per chip. The image is accumulated over the whole chip. After integration, charges are shifted towards output register, one row at a time, and each line is read-out between row shifts.

2.6 *Small Window (pn imaging mode)*

As a baseline we choose a window size is 48×30 pixels, located in a corner of a given chip. Only the pixels within such window are read-out, and the information from the remaining part of the chip is lost. The other 11 chips are operating in the FF mode. It will take us 0.6 ms to read-out such a window, and the read-out time of one of the other chips, which is 4 ms, is used as exposure time for the window CCD: thus the frame time will be 4.6 ms.

2.7 *Large Window (pn imaging mode)*

It is also possible to select a larger window, which overlaps several CCDs. For example, a window which covers 1/4 of the focal plane area, could be read within 11 ms. The other part of the focal plan area is not analysed.

This mode has not yet been simulated.

2.8 *Timing (pn timing mode)*

Only one source of significance must be in the field using this mode. 20 pixels of each of the 64 columns are integrated before conversion, along the transfer direction in 20 μs; the information from this strip of 20×64 pixels is then converted and read-out in 20 μs. In this mode, the target source is continuously monitored, with a time resolution of 40 μs, but there is an increase of the effective pixel size of a factor of 20 trading positional for temporal information. In this mode only a single chip is read-out, the other chips are not read-out at all. The result of this scheme is similar to that of the MT.

2.9 Burst (pn timing mode)

The target image should be placed in the top 10 rows of the chip (191 to 200), i.e. the ones farthest from the read-out register. While this top part is exposed, the remaining part of the CCD is used as an analogue storage. Image charges are transfered continuously to the output nodes with a frequency of 1 MHz. After 0.2 ms the image taken in the first microsecond (row 200) has been shifted 200 lines down. During read-out, the data stored in rows 1 to 190 will be sampled in 20 μs per row (3.8 ms). During this time pixels in row 191 to 200 will still be over-exposed to the source. Events from these rows must therefore be discarded. Thus the frame time is 4 ms, with a duty cycle of 4.8% (i.e. 0.19 ms/4 ms). In this mode only a single chip is read-out, the other chips are not read-out at all. This mode, quite similar to RFS, gives a time resolution of 20 μs and permits pointing at very bright sources.

3. Simulations

The simulations have been pursued using the EPOS software package (Chiappetti 1994b), available at IFCTR, Milano. The procedure applied is as follows.

A monochromatic set of N photons of a given energy is generated with random positions following a bivariate normal distribution (σ = 12.72") as an energy-independent approximation of the on-axis mirror point spread function (PSF). An arrival time is assigned to each photon according to a given temporal distribution (a constant one in the simplest case); the effect of filters and dead layers in the chip are neglected at this stage. The coordinates of the photon are converted from microns in the focal plane to pixels on a chip, and then this photon list is submitted to the CCD detection simulation package. Finally, the read-out, pattern recognition, controller and (for the pn) on-ground event reconstruction and thresholding procedures are simulated for each operating mode. From the resulting photon file, a spectrum is accumulated. The two main problems connected with images and spectra reconstruction are splitting and pile-up.

The first effect is due to the fact that a photon interacting with the silicon of the CCDs, produces hole-electron pairs in more than one pixel. In this case we have to sum all the charges in order to recover correctly the entire energy of the X-ray (event reconstruction, done in the onboard controller or on ground).

The pile-up effect is the overlapping of more than one photon in the same pixel (physical pile-up) or in adjacent pixels (geometrical pile-up); in the second case some events could be reconstructed by pattern analysis, but to overcome the whole problem one has to limit the observable source intensity. The aim of these simulations is to find a quantitative criterion for

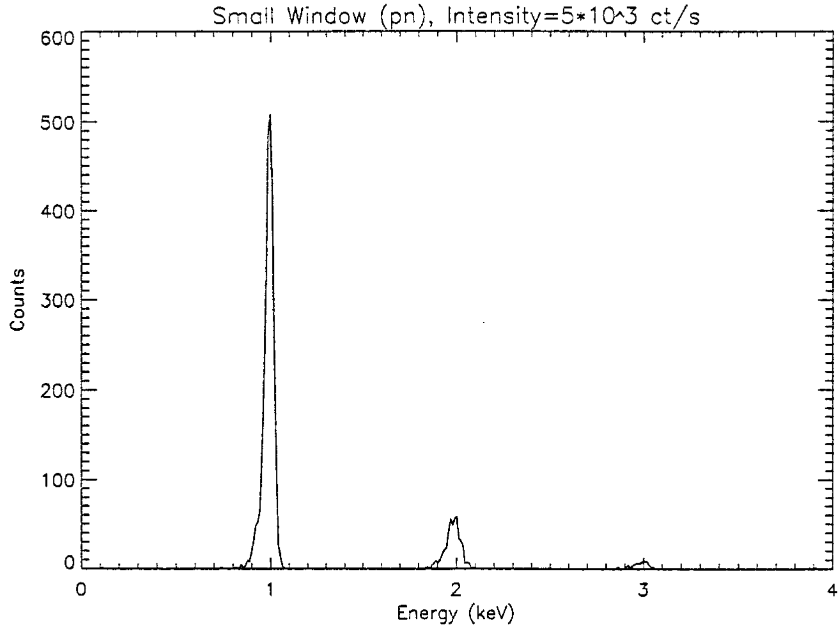

Fig. 2. The spectrum of a monochromatic line ($E = 1\ keV$) after read-out and controller reconstruction: the events at 2 and 3 keV are due to pile-up.

setting a threshold for the maximum value of the observable source intensity, as a function of the read-out mode. To define the maximum acceptable pile-up rate, we extract from the accumulated monochromatic spectra the number of photons which are affected by the pile-up, i.e. which have an energy at least double the original (Fig.2); then we divide this number by the total number of reconstructed photons at the end of the whole simulation chain. We analyse the pile-up rate for different values of the intensity of the observed sources, and also for different energies.

In this context, the problem of X-ray and charged particle background rejection has not been carried on.

4. Results

In the following we list, in the form of one table for each read-out mode, the ratios of the piled-up to the total number of photons reconstructed at the end of the whole simulation chain, for different intensities (in ct/s) at different energies. The reason why we performed simulations at different energies is that, even if our PSF is energy-independent, the photon splitting depends on energy and it could affect the pile-up rates.

Frame Store (MOS) (% pile-up)

I (ct/s)	0.1 keV	0.5 keV	1.0 keV	2.0 keV	4.0 keV	6.0 keV	average
11	5.0	5.4	5.0	5.0	4.2	2.7	4.55
8	3.5	4.0	3.6	3.6	3.0	1.8	3.25
6	2.4	2.7	2.4	2.5	2.2	1.1	2.22
4	2.1	2.2	1.9	2.0	1.7	1.0	1.82
2	1.1	1.2	1.1	1.1	1.0	0.5	1.00

Window Frame Store (MOS) (% pile-up)

I (ct/s)	0.1 keV	0.5 keV	1.0 keV	2.0 keV	4.0 keV	6.0 keV	average
260	6.0	6.8	6.1	6.0	5.0	3.6	5.58
130	2.5	2.8	2.6	2.6	2.3	1.2	2.33
100	2.4	2.6	2.4	2.4	2.1	1.4	2.22
70	1.7	1.9	1.8	1.8	1.6	1.0	1.63
40	1.1	1.2	1.2	1.2	1.0	0.7	1.07

Refresh Frame Store (MOS) (% pile-up)

I (ct/s)	0.1 keV	0.5 keV	1.0 keV	2.0 keV	4.0 keV	6.0 keV	average
1300	13.3	15.7	14.5	14.7	11.1	11.0	13.38
800	8.2	8.7	8.2	8.1	6.4	4.5	7.35
520	6.1	6.6	6.6	6.7	5.4	3.8	5.87
260	4.8	4.7	4.4	4.4	3.9	3.3	4.25
130	1.4	1.5	1.4	1.4	1.1	0.8	1.27

Timing (MOS) (% pile-up)

I (ct/s)	0.1 keV	0.5 keV	1.0 keV	2.0 keV	4.0 keV	6.0 keV	average
1730	5.0	5.6	5.5	5.6	5.2	5.0	5.32
1300	3.9	4.1	4.1	4.1	4.0	3.6	3.97
870	2.2	2.5	2.4	2.5	2.4	2.1	2.35
390	1.5	1.5	1.5	1.5	1.5	1.3	1.47
130	0.7	0.6	0.6	0.6	0.6	0.4	0.58

Full Frame (pn) (% pile-up)

I (ct/s)	0.1 keV	0.5 keV	1.0 keV	2.0 keV	4.0 keV	6.0 keV	average
60	5.6	5.9	5.2	4.5	4.6	4.7	5.08
46	4.0	4.2	3.6	2.9	3.2	3.4	3.55
38	3.3	3.3	2.9	2.5	2.6	2.7	2.88
26	2.1	2.3	2.0	1.9	2.0	2.0	2.05
13	1.3	1.1	1.0	1.1	1.1	1.1	1.12

Small Window (pn) (% pile-up)

I (ct/s)	0.1 keV	0.5 keV	1.0 keV	2.0 keV	4.0 keV	6.0 keV	average
650	5.8	5.7	5.0	4.7	4.7	5.0	5.15
520	4.2	4.8	4.0	3.7	3.7	3.9	4.05
325	2.3	2.9	2.5	2.1	2.3	2.3	2.40
130	1.2	1.4	1.2	1.1	1.1	1.1	1.18

Timing (pn) (% pile-up)

I (ct/s)	0.1 keV	0.5 keV	1.0 keV	2.0 keV	4.0 keV	6.0 keV	average
10400	9.1	9.4	9.2	9.0	8.5	9.0	9.03
8600	4.3	4.7	4.6	4.6	4.5	4.5	4.53
5200	2.9	3.3	3.2	3.2	3.1	3.1	3.13
3900	1.7	1.9	1.9	1.9	1.9	1.9	1.87
1300	0.6	0.8	0.8	0.8	0.8	0.8	0.77

Burst (pn) (% pile-up)

I (ct/s)	0.1 keV	0.5 keV	1.0 keV	2.0 keV	4.0 keV	6.0 keV	average
50000	5.1	4.0	3.5	2.8	3.0	3.8	3.70
20000	2.0	2.5	2.2	1.7	1.4	1.7	1.92
10000	0.8	0.6	0.6	0.6	0.5	1.0	0.68
1000	0.2	0.2	0.2	0.2	0.2	0.2	0.20

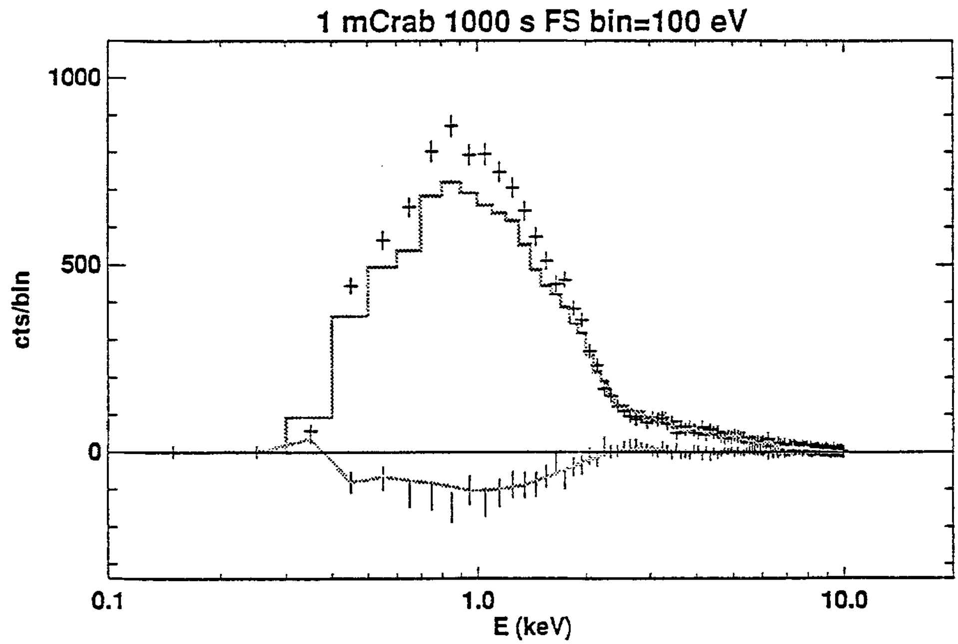

Fig. 3. A typical simulated Crab-like spectrum. The crosses are the source spectrum, while the line is the reconstructed one; also the residuals are shown.

5. Limiting rates

From the pile-up rates derived in the previous simulations, it is now possible to look for the maximum value of the intensity of the sources observable by EPIC, with the different read-out modes.

First of all, we compare the results of these simulations with those obtained with simulated Crab-like spectra (Chiappetti 1994a). A typical spectrum is shown in Fig.3.

In the former case, a realistic spectrum of given intensity was submitted to the whole chain of simulation, and then the output was compared with the input spectrum. The simulations have been done for the various source intensities for a different exposure time, such that the overall photon statistics were the same, and of quality comparable to the spectrum in Fig.3. To define the limiting rate for the intensity, the following quantities were introduced.

If P_i is the input spectrum and O_i is the reconstructed output spectrum, and both are accumulated as count histograms with poissonian errors $\sigma_{P_i} = \sqrt{P_i}$ and $\sigma_{O_i} = \sqrt{O_i}$, then it is quite natural to define the residuals and their errors as:

$$R_i = O_i - P_i, \qquad \sigma_{R_i} = \sqrt{\sigma_{O_i}^2 + \sigma_{P_i}^2} = \sqrt{O_i + P_i}.$$

If all the input photons splitted into more than one event were reconstructed back into one photon, one would expect the residuals to be distributed around an expected value of zero. The noise in the residuals will be due just to the effects of the energy resolution and of the low charge threshold.

At this point the total residual and its error can be computed, as follows:

$$R_{tot} = \sum_i R_i, \qquad \sigma_{tot} = \sqrt{\sum_i \sigma_{R_i}^2};$$

from these two quantities the significance $S = R_{tot}/\sigma_{tot}$ can be defined. A possible quantitative criterion to find the limiting rate is to set a threshold for the intensity of the source roughly around the case $S = 5$ (5-sigma significance of the overall residual). This criterion is relevant to the simulation conditions as described above.

Moreover the χ^2 of the residuals around their expected value (i.e. zero) is defined as follows:

$$\chi^2 = \sum_{R_i \neq 0} (\frac{R_i}{\sigma_i})^2,$$

and can be used to check the goodness of spectral reconstruction. A good agreement is found among the two methods and the visual inspection of spectra, and thus the 5-sigma significance criterion will be considered in the following, for sake of simplicity.

Read-out mode	I (ct/s) at $S = 5$	% pile-up Minimum	Maximum	Average
FS	7	1.5	3.4	2.7
WFS	110	1.3	2.7	2.2
RFS	900	6.8	10.5	9.2
MT	1020	2.8	3.5	3.2
FF	27	1.9	2.4	2.2
SW	550	3.9	5.0	4.3
PT	>10000	8.5	9.4	9.0
B	>20000	1.4	2.5	1.9

Table 1: Pile-up percentages for each read-out mode, corresponding to the $S = 5$ criterion (Chiappetti 1994a).

To quickly compare the results of the two simulation methods, in Table 1 we list, for each mode, the intensity I (in ct/s) corresponding to S = 5 (Chiappetti 1994a) and the percentage of pile-up events (there are the minimum, the maximum and the average values, extracted from the previous tables).

From Table 1 a certain difference appears between the two methods: the pile-up rates corresponding to $S = 5$ are quite different for different modes. For some of them, e.g. RFS and PT, the threshold at $S = 5$ corresponds to pile-up rates which are unacceptably high.

Another way to use these results is to define a pile-up rate limit, and to look for the corresponding maximum value of the intensity (in ct/s) for each mode. In Table 2, the maximum intensity values are given, for both types of CCD, corresponding to pile-up rates of 1%, 2% and 5% respectively.

Read-out	Intensity (ct/s)		
mode	1% pile-up	2% pile-up	5% pile-up
FS	2	4	12
WFS	40	90	215
RFS	130	160	430
MT	280	700	1620
FF	10	26	66
SW	100	260	625
PT	1700	4000	8750
B	12500	25400	>50000

Table 2: Intensity thresholds for different pile-up percentages.

These thresholds should be considered as a first step in determining the intensity limits for the observable sources. Starting from this point we can now look to the real sky in order to understand the impact of the different read-out modes on the scientific objectives of the mission.

6. The real sky

From a scientific point of view, it is very important to know which are the sources that could be pointed by EPIC when it is set in a particular read-out mode, and how many of these sources could be observed in any part of the

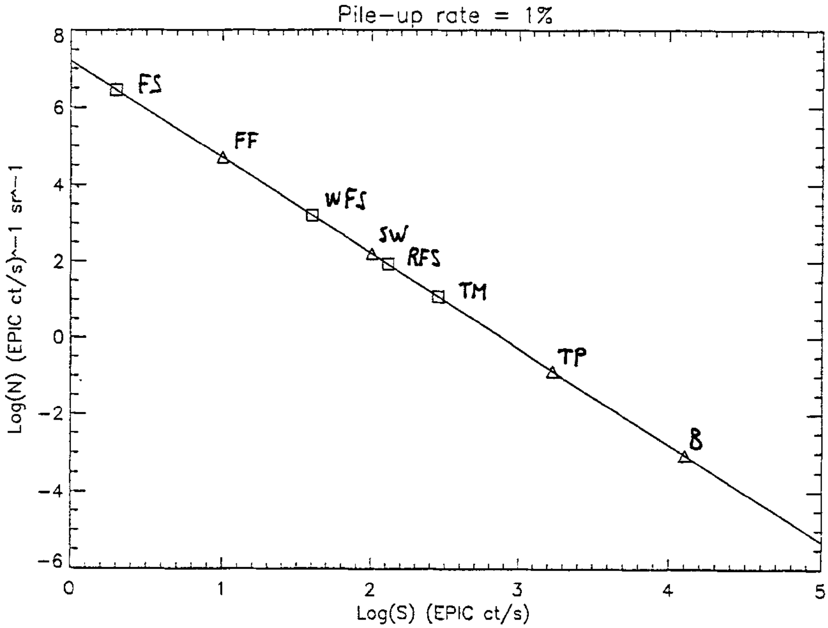

Fig. 4. Log$N$-log$S$ distribution for non-galactic objects and the read-out mode thresholds corresponding to pile-up rates of 1%.

sky, for a given pile-up rate. In the following, we shall fix the pile-up rate at the values of 1% (and 5%).

At this point some comments are in order:

In order to make this analysis, we need a number-intensity distribution (log$N$-log$S$) for X-ray sources in the EPIC energy band (0.1-10 keV). The best one available for our purpose is still that constructed by Piccinotti et al. (1982) from the HEAO-1 experiment A-2; this experiment permitted the creation of a complete catalog of X-ray sources at galactic latitudes $|b| > 20^o$ down to a limiting sensitivity of 3.1×10^{-11} $erg/cm^2/s$ in the 2-10 keV band. The completeness of the sample examined enabled the authors to construct a log$N$-log$S$ relation for non-galactic objects, which is consistent with the results of previous experiments, such as Uhuru (Schwartz 1979) and Ariel 5 (Warwick and Pye 1978).

This relation can be written as:

$$N(S) \sim 16.5\ S^{-2.5}(ct_{\rm R15}/s)^{-1}\ sr^{-1}, \tag{1}$$

where 1 $ct_{\rm R15}/s$ corresponds to $\sim 2.4 \times 10^{-11}$ $erg/cm^2/s$ (Piccinotti et al. 1982).

On the other hand, 1 $ct_{\rm EPIC}/s$ corresponds to $\sim 2.7 \times 10^{-13}$ $erg/cm^2/s$ in the same energy band, which leads to a conversion factor between EPIC and R15 counts of $\sim 1.12 \times 10^{-2}$ for the same, standard, Crab-like spectra.

Thus the number-intensity relation in EPIC units becomes:

$$N(S) \sim 1.27 \times 10^6 \ S^{-2.5} (ct_{\rm EPIC}/s)^{-1} \ sr^{-1}. \qquad (2)$$

Fig.4 shows the threshold values for the different read-out modes corresponding to the pile-up rate of 1%, superimposed on the log$N$-log$S$ distribution.
• the total number of (non-galactic) sources detectable by EPIC all over the sky (in the 2-10 keV band), with $S \geq 1 \ ct_{\rm EPIC}/s$, is $\sim 1.6 \times 10^7$;

• if we only use the imaging modes FS, WFS, RFS, FF and SW, a number of $\sim 10^4$ bright sources cannot be pointed at in the case of 1% maximum pile-up rate ($\sim 10^3$ in the case of 5% maximum pile-up rate);

• with all the read-out modes available, particularly the Burst one, we can point at sources with intensity up to $S \leq 12500 \ ct_{\rm EPIC}/s$, and this means that only ~ 10 sources observed by EPIC will give a pile-up rate $\geq 1\%$.

From these simple considerations follows the importance of several read-out modes for the completeness and the flexibility of the EPIC mission science. In fact, even if EPIC will enable, by virtue of its high throughput and using simple read-out modes, detection of many more faint X-ray sources than in previous missions, on the other hand, in order not to lose the spectroscopy and timing analysis of the brightest sources, it will be necessary to make use of more complex read-out modes.

References

Bignami G.F. et al.: 1989, 'EPIC: European (X-ray) Photon Imaging Camera', *proposal submitted to ESA for the XMM cornerstone mission* ,

Chiappetti L. et al.: 1993, 'EPIC Operating Modes', *EPIC project, report of the Operating Mode Working Group* , EPIC-IFC-TN-001

Chiappetti L.: 1994a, 'A re-assessment of EPIC telemetry rates', *EPIC project technical note* , EPIC-IFC-TN-005

Chiappetti L.: 1994b, 'EPOS: EPic Observation Simulations', *EPIC project technical note* , EPIC-IFC-TN-006

Lumb D.H., Berthiaume G.D., Burrows D.N., Garmire G.P., Nousek J.A.: 1991, *Exp. Astr.* **2**, 179

Piccinotti G. et al.: 1982, *ApJ* **253**, 485

Pigot C.: 1993, 'Some comments on operating modes', , private comunication

Sarra P.F., Bignami G.F.: 1993, *Exp. Astr.* **2**, 357

Schwartz D.A.: 1979, 'X-Ray Astronomy' in Proceedings of the 21th Plenary Meeting of the Committee on Space Research, ed(s)., *W.A.Baity and L.E.Peterson*, N.Y.:Pergamon, pag. 453

Strüder L.: 1994, 'Semiconductor-X-Ray detectors' in Proceedings of the 4^{th} Course of the International School of Space Science, ed(s)., *S. Massaglia*, L'Aquila, in press

Turner M.: 1994, 'CCDs in X-Ray Spectroscopy: promise and realisation' in Proceedings of the 4^{th} Course of the International School of Space Science, ed(s)., *S. Massaglia*, L'Aquila, in press

Warwick R.S. and Pye J.P.: 1978, *MNRAS* **183**, 169